

## Stereochemistry and Stereochemical Rearrangements of Eight-Coordinate Tetrakis Chelates. 2. Preparation, Characterization, and Structure of Tetrakis(thioacetylacetonato)zirconium(IV)<sup>1</sup>

MICHAEL E. SILVER, HEI KYUNG CHUN, and ROBERT C. FAY\*

Received February 2, 1982

Tetrakis(thioacetylacetonato)zirconium(IV), [Zr(Sacac)<sub>4</sub>], has been prepared by reaction of stoichiometric amounts of zirconium(IV) chloride and Na(Sacac) in dichloromethane and has been characterized by infrared and <sup>1</sup>H NMR spectra. The crystal and molecular structure of [Zr(Sacac)<sub>4</sub>] has been determined by X-ray diffraction and has been refined anisotropically by least-squares methods to  $R_1 = 0.040$  and  $R_2 = 0.048$  using 2651 independent diffractometer data having  $2\theta_{MoK\alpha} \leq 44.0^\circ$  and  $|F_o| \geq 2.0\sigma_F$ . The compound crystallizes in the monoclinic space group  $P2_1/n$  with four molecules in a unit cell having dimensions  $a = 8.562$  (1) Å,  $b = 25.112$  (4) Å,  $c = 11.742$  (2) Å, and  $\beta = 91.84$  (1)° ( $\rho_{obsd} = 1.45$  g cm<sup>-3</sup>,  $\rho_{calcd} = 1.453$  g cm<sup>-3</sup>). The crystal contains discrete eight-coordinate molecules in which the bidentate thioacetylacetonate ligands span the *s* edges of a (necessarily distorted)  $D_{4d}82m$  square antiprism. The unsymmetrical ligands are arranged so as to cluster the sulfur atoms in all-cis positions. The observed square-antiprismatic *ssss*-C<sub>2</sub> stereoisomer is distorted in the direction of the dodecahedral *mmgg*-C<sub>1</sub> and bicapped-trigonal-prismatic  $t_1t_1p_2p_2$ -C<sub>1</sub> stereoisomers. Consistent with the former distortion, the averaged Zr-O and Zr-S bond lengths fall into two classes: Zr-O<sub>A</sub> = 2.185 Å; Zr-O<sub>B</sub> = 2.132 Å; Zr-S<sub>A</sub> = 2.724 Å; Zr-S<sub>B</sub> = 2.665 Å. One of the chelate rings exhibits an unusual ring folding direction; it is bent toward the quasi-8 axis of the antiprism. Low-temperature <sup>1</sup>H NMR spectra of [Zr(Sacac)<sub>4</sub>] in CHClF<sub>2</sub> exhibit just two methyl resonances down to -163 °C.

### Introduction

The first examples of "stereochemically rigid" eight-coordinate tetrakis chelates have been reported recently. Examples include (1) tetrakis( $\beta$ -diketonates), [M(dik)<sub>4</sub>] (M = Zr, Hf, U),<sup>2-4</sup> (2) the W(IV) mixed-ligand complexes [W(mpic)<sub>3</sub>(dcq)] and [W(mpic)<sub>2</sub>(dcq)<sub>2</sub>] (mpic = 5-methylpicolinate and dcq = 5,7-dichloro-8-quinolinolate),<sup>5,6</sup> (3) the tetrakis(*N,N*-dimethyldithiocarbamato)tantalum(V) cation, [Ta(S<sub>2</sub>CNMe<sub>2</sub>)<sub>4</sub>]<sup>+</sup>,<sup>7</sup> and (4) the *N,N*-dimethylmonothiocarbamate complexes [M(SOCNMe<sub>2</sub>)<sub>4</sub>] (M = Ti, Zr).<sup>8</sup> The monothiocarbamate complexes are particularly interesting because (1) they appear to be more rigid than the carbamate<sup>9</sup> and dithiocarbamate<sup>10-13</sup> analogues and (2) they have dodecahedral structures in which the four sulfur atoms cluster in all-cis positions on one side of the coordination polyhedron.<sup>14</sup> The sulfur and oxygen atoms do not sort between the dodecahedral A and B sites, as predicted by Orgel's rule.<sup>15</sup>

In an effort to learn whether clustering of sulfur atoms is common in eight-coordinate complexes that contain unsymmetrical sulfur-donor ligands, and in order to explore the relationship between sulfur atom clustering and stereochemical rigidity, we have begun to investigate early-transition-metal chelates with other unsymmetrical sulfur-donor ligands. In this paper, we report the synthesis, X-ray crystal structure, and low-temperature NMR spectra of tetrakis(thioacetylacetonato)zirconium(IV), [Zr(Sacac)<sub>4</sub>]. Although thio- $\beta$ -

diketonate complexes of later transition metals have been studied extensively,<sup>16,17</sup> early-transition-metal thio- $\beta$ -diketonates have been largely neglected and, to our knowledge, no zirconium complexes have been reported.

### Experimental Section

**Reagents and General Techniques.** Sodium thioacetylacetonate, Na(Sacac), was prepared as described elsewhere<sup>18</sup> and dried in vacuo for 24 h. Zirconium(IV) chloride (Alfa Products) was used without further purification. Chlorodifluoromethane (Freon 22, Matheson Gas Products) was dried by passage through a column containing phosphorus(V) oxide. Hexane and dichloromethane were dried by refluxing over calcium hydride and phosphorus(V) oxide, respectively, for at least 24 h and were distilled immediately before use. Syntheses and subsequent handling of Na(Sacac) and [Zr(Sacac)<sub>4</sub>] were conducted under anhydrous conditions under a dry nitrogen atmosphere.

**Tetrakis(4-mercaptopent-3-en-2-onato)zirconium(IV), [Zr(Sacac)<sub>4</sub>].** This complex was prepared by reaction of zirconium(IV) chloride (1.60 g, 6.87 mmol) and Na(Sacac) (4.00 g, 29.0 mmol) in dichloromethane (120 mL) at room temperature. After 0.5 h, the reaction mixture was filtered, yielding a clear, orange filtrate. Solvent removal via trap-to-trap vacuum distillation resulted in an orange solid, which was dried in vacuo for 8 h; yield 3.22 g (85%). Slow cooling of a hot hexane-dichloromethane (~5:1 v/v) solution of this solid afforded orange crystals, mp 145-147 °C. Anal. Calcd for Zr-(C<sub>5</sub>H<sub>7</sub>OS)<sub>4</sub>: C, 43.52; H, 5.11; Zr, 16.53. Found: C, 43.44; H, 5.05; Zr, 16.74. <sup>1</sup>H NMR (CDCl<sub>3</sub> solution, 34 °C): -2.07 (CH<sub>3</sub>), -2.39 (CH<sub>2</sub>), and -6.38 ppm (CH) relative to an internal reference of tetramethylsilane (1% by volume).

**Nuclear Magnetic Resonance Spectra.** Proton chemical shifts were measured at ambient probe temperature (~34 °C) with a Varian EM-390 90-MHz spectrometer. The sweep width was calibrated with a sample of chloroform-*d*, 99.8 atom % deuterium, and tetramethylsilane.

Variable-temperature continuous-wave <sup>1</sup>H NMR spectra of a 0.036 M solution of [Zr(Sacac)<sub>4</sub>] in chlorodifluoromethane (Freon 22) were recorded in the temperature range -61.0 to -163.0 °C with a Bruker HX-90 spectrometer which was locked on the solvent proton resonance. Temperatures, determined with a copper-constantan thermocouple immersed in acetone, are estimated to be accurate to  $\pm 0.5$  °C.

**Infrared Spectra.** Infrared spectra were recorded in the region 4000-300 cm<sup>-1</sup> with a Perkin-Elmer 521 grating spectrophotometer.

- (1) Presented in part at the Symposium on the Inorganic and Bioinorganic Chemistry of Sulfur Complexes, 179th National Meeting of the American Chemical Society, Houston, TX, March 1980.
- (2) Fay, R. C.; Howie, J. K. *J. Am. Chem. Soc.* **1977**, *99*, 8110.
- (3) Fay, R. C.; Howie, J. K. *J. Am. Chem. Soc.* **1979**, *101*, 1115.
- (4) Kiener, C.; Folcher, G.; Langlet, G.; Rigny, P.; Virlet, J. *Nowv. J. Chim.* **1979**, *3*, 99.
- (5) Archer, R. D.; Donahue, C. J. *J. Am. Chem. Soc.* **1977**, *99*, 269.
- (6) Donahue, C. J.; Archer, R. D. *J. Am. Chem. Soc.* **1977**, *99*, 6613.
- (7) Fay, R. C.; Lewis, D. F.; Weir, J. R. *J. Am. Chem. Soc.* **1975**, *97*, 7179.
- (8) Hawthorne, S. L.; Bruder, A. H.; Fay, R. C. *Inorg. Chem.* **1978**, *17*, 2114.
- (9) Chisholm, M. H.; Extine, M. W. *J. Am. Chem. Soc.* **1977**, *99*, 782.
- (10) Bradley, D. C.; Giltz, M. H. *J. Chem. Soc. A* **1969**, 1152.
- (11) Muetterties, E. L. *Inorg. Chem.* **1973**, *12*, 1963.
- (12) Muetterties, E. L. *Inorg. Chem.* **1974**, *13*, 1011.
- (13) Bhat, A. N.; Fay, R. C.; Lewis, D. F.; Lindmark, A. F.; Strauss, S. H. *Inorg. Chem.* **1974**, *13*, 886.
- (14) Steffen, W. L.; Fay, R. C. *Inorg. Chem.* **1978**, *17*, 2120.
- (15) Orgel, L. E. *J. Inorg. Nucl. Chem.* **1960**, *14*, 136.

- (16) (a) Cox, M.; Darken, J. *Coord. Chem. Rev.* **1971**, *7*, 29. (b) Livingstone, S. E. *Ibid.* **1971**, *7*, 59.
- (17) Mehrotra, R. C.; Bohra, R.; Gaur, D. P. "Metal  $\beta$ -Diketonates and Allied Derivatives"; Academic Press: New York, 1978; Chapter 5.
- (18) Siiman, O.; Fresco, J. *J. Chem. Phys.* **1971**, *54*, 734.

The compounds were studied as Nujol mulls supported between cesium iodide plates. The estimated uncertainty in reported frequencies is  $\pm 4 \text{ cm}^{-1}$ .

**Crystallography.** Several orange crystals of  $[\text{Zr}(\text{Sacac})_4]$  were sealed under dry nitrogen in 0.5-mm Lindemann capillaries. Weissenberg and precession photographs indicated the crystal system to be monoclinic, and the systematically absent reflections ( $h0l$  for  $h + l \neq 2n$  and  $0k0$  for  $k \neq 2n$ ) identified the space group as  $P2_1/n$ . The lattice constants of  $a = 8.562$  (1) Å,  $b = 25.112$  (4) Å,  $c = 11.742$  (2) Å, and  $\beta = 91.84$  (1)° were determined by least-squares refinement of the diffraction geometry for 15 reflections ( $2\theta > 14.25^\circ$ ) centered on a computer-controlled four-circle Syntex  $P2_1$  diffractometer using graphite-monochromated Mo  $K\alpha$  radiation ( $\lambda = 0.71069$  Å). The calculated density based on four molecules of  $[\text{Zr}(\text{C}_5\text{H}_7\text{OS})_4]$  per unit cell is  $1.453 \text{ g cm}^{-3}$ ; the observed density, measured by flotation with a solution of carbon tetrachloride and hexane, was  $1.45 \text{ g cm}^{-3}$ .

A rectangular-shaped prism of dimensions  $0.35 \times 0.21 \times 0.17 \text{ mm}$  was chosen for collection of intensity data. The data were collected on the Syntex  $P2_1$  diffractometer with use of the  $\theta$ - $2\theta$  scan technique with graphite-monochromated Mo  $K\alpha$  radiation at a takeoff angle of  $6.3^\circ$  and a glancing angle of  $2.5^\circ$ . A variable scan rate ranging from  $2^\circ \text{ min}^{-1}$  in  $2\theta$  for reflections of intensity  $\leq 150 \text{ counts s}^{-1}$  to  $29.3^\circ \text{ min}^{-1}$  for reflections of intensity  $\geq 1500.0 \text{ counts s}^{-1}$  was employed. The range of each scan consisted of a base width of  $2.0^\circ$  at  $2\theta = 0^\circ$  and an increment of  $\Delta(2\theta) = (0.692 \tan \theta)^\circ$  to allow for spectral dispersion; background counts of duration equal to half the total scan time were taken at both limits of the scan. Reflections with intensities greater than  $50\,000 \text{ counts s}^{-1}$  were flagged as being too intense to measure and were recollected at lower tube current settings. The intensities of three standard reflections, measured at 63-reflection intervals to monitor the stability of the system, gave no indication of misalignment or deterioration of the crystal.

A total of 3454 unique reflections having  $2\theta \leq 44.0^\circ$  (0.60 times the number of data in the limiting Cu  $K\alpha$  sphere) was scanned. On the basis of the cited dimensions of the crystal and a linear absorption coefficient of  $7.69 \text{ cm}^{-1}$ , the maximum error resulting from neglect of absorption corrections was estimated to be  $< 2.9\%$  in any intensity and  $< 1.5\%$  in any structure amplitude. Therefore absorption corrections were judged unnecessary. The intensity data were reduced to a set of relative squared amplitudes,  $|F_o|^2$ , by the application of standard Lorentz and polarization factors. Those 2651 reflections having  $|F_o| > 2.0\sigma_F$ , where  $\sigma_F$  is defined elsewhere,<sup>19</sup> were retained as "observed" for the structure analysis.

**Structure Determination and Refinement.** The structure was solved by application of Patterson and Fourier techniques and was refined by full-matrix least-squares minimization of the function  $\sum w(|F_o| - |F_c|)^2$ , where  $w = 1/\sigma_F^2$  is a weighting factor. Anomalous dispersion corrections for the Zr and S atoms and anisotropic thermal parameters for all non-hydrogen atoms were employed. Refinement of the positional and thermal parameters of the 29 non-hydrogen atoms followed by a difference Fourier synthesis permitted location of the 28 hydrogen atoms. Hydrogen atom coordinates were then calculated on the basis of the C atom positions and a C-H bond length of 1.0 Å. The H atoms were assigned isotropic thermal parameters by adding  $1.0 \text{ Å}^2$  to the equivalent isotropic thermal parameter of the attached C atom. Further cycles of refinement with fixed positional and thermal parameters for the H atoms led to discrepancy indices  $R_1 = 0.040$  and  $R_2 = 0.048$ , where

$$R_1 = \sum ||F_o| - |F_c|| / \sum |F_o|$$

$$R_2 = [\sum w(|F_o| - |F_c|)^2 / \sum w|F_o|^2]^{1/2}$$

In the final cycle of refinement no parameter varied by more than 0.04 (the average was 0.01) of its estimated standard deviation. A final difference Fourier showed no anomalous features; the strongest peak had a density of  $0.41 \text{ e Å}^{-3}$ .

Scattering factors were taken from Cromer and Mann<sup>20</sup> for  $\text{Zr}^0$ ,  $\text{S}^0$ ,  $\text{O}^0$ , and  $\text{C}^0$  and from Stewart, Davidson, and Simpson<sup>21</sup> for  $\text{H}^0$ . Anomalous dispersion corrections, real and imaginary, for Zr and S were obtained from Cromer.<sup>22</sup> Calculations were performed on

**Table I.** Characteristic Infrared Frequencies ( $\text{cm}^{-1}$ ) for  $[\text{Zr}(\text{Sacac})_4]$  and  $\text{Na}(\text{Sacac})^a$

$[\text{Zr}(\text{Sacac})_4]$	$\text{Na}(\text{Sacac})$	predominant mode <sup>b</sup>
1546 s <sup>c</sup>	1600 s 1568 w	$\nu(\text{C}-\text{O})$
1493 <sup>d</sup> s		$\nu(\text{C}-\text{C})$
1431 <sup>d</sup> w	1430 <sup>d</sup> w	$\text{CH}_3$ deg def
1368 <sup>d</sup> w	1353 w 1341 w	$\text{CH}_3$ sym def
1321 m	1318 m 1249 vw	$\delta(\text{C}-\text{H})$
1241 s	1197 s	$\nu(\text{C}-\text{C}) + \nu(\text{C}-\text{CH}_3)$
1122 m	1108 m	$\nu(\text{C}-\text{CH}_3)$
1021 m	1002 s	$\text{CH}_3$ rock
994 sh	967 w	
944 m	915 m	$\nu(\text{C}-\text{CH}_3)$
828 m	782 s	$\pi(\text{C}-\text{H})$
814 m		
804 m		
730 s	705 m	$\nu(\text{C}-\text{S})$
629 s	605 s	$\nu(\text{M}-\text{O}) + \text{ring def} + \delta(\text{C}-\text{CH}_3)$
509 m	509 m	$\delta(\text{C}-\text{CH}_3) + \text{ring def}$
472 m		$\nu(\text{Zr}-\text{O})$
362 s		$\nu(\text{Zr}-\text{S})$
e	353 w	$\delta(\text{C}-\text{CH}_3)$
330 w	326 w	ring def

<sup>a</sup> As Nujol mulls between CsI plates; 2000–300- $\text{cm}^{-1}$  region.

<sup>b</sup> Legend:  $\nu$ , stretch;  $\delta$ , in-plane deformation;  $\pi$ , out-of-plane deformation. Assignments are based on ref 18 and 23.

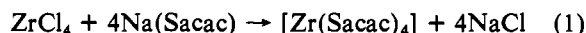
<sup>c</sup> Abbreviations: s, strong; m, medium; w, weak; v, very; sh, shoulder. <sup>d</sup> These frequencies are somewhat uncertain because the absorption bands are partially obscured by Nujol bands.

<sup>e</sup> Obscured by a strong band at  $362 \text{ cm}^{-1}$ .

PRIME 300 and IBM 370/168 computers using programs listed in a previous paper.<sup>14</sup>

## Results and Discussion

**Preparation and Properties of  $[\text{Zr}(\text{Sacac})_4]$ .** Tetrakis(thioacetylacetonato)zirconium(IV),  $[\text{Zr}(\text{Sacac})_4]$ , has been prepared in good yield by reaction of stoichiometric amounts of zirconium(IV) chloride and sodium thioacetylacetonate in dichloromethane:



Recrystallization from hot hexane-dichloromethane afforded a product of good purity as judged by satisfactory elemental analysis and  $^1\text{H}$  NMR spectra (see Experimental Section).

$[\text{Zr}(\text{Sacac})_4]$  is soluble in dichloromethane and chloroform but essentially insoluble in saturated hydrocarbons. The complex is thermally stable, and its infrared spectrum exhibits no evidence of hydrolysis after exposure of the solid to the atmosphere for 48 h. Solutions, however, are less stable toward hydrolysis; NMR spectra indicate appreciable hydrolysis within 30 min.

Characteristic infrared frequencies for  $[\text{Zr}(\text{Sacac})_4]$  and  $\text{Na}(\text{Sacac})$  are listed in Table I along with suggested assignments, which are based on previously published normal-coordinate analyses of the vibrations of several divalent metal thioacetylacetonates.<sup>18,23</sup> The band at  $472 \text{ cm}^{-1}$  in the spectrum of  $[\text{Zr}(\text{Sacac})_4]$ , not present in the spectrum of  $\text{Na}(\text{Sacac})$ , is tentatively assigned to a Zr-O stretching mode. This frequency is higher than  $\nu(\text{Zr}-\text{O})$  in  $\text{Zr}(\text{acac})_4$  ( $421 \text{ cm}^{-1}$ ),<sup>24</sup> perhaps due to the shorter Zr-O bond length in  $\text{Zr}(\text{Sacac})_4$  (vide infra) and/or coupling of Zr-O and Zr-S stretching modes. Assignment of the  $362\text{-cm}^{-1}$  band to  $\nu(\text{Zr}-\text{S})$  is less certain. This band is much stronger than the weak  $353\text{-cm}^{-1}$  band in the spectrum of  $\text{Na}(\text{Sacac})$ , and its frequency agrees well with  $\nu(\text{Zr}-\text{S})$  in tetrakis(dithio-

(19) Radonovich, L. J.; Bloom, A.; Hoard, J. L. *J. Am. Chem. Soc.* **1972**, *94*, 2073.

(20) Cromer, D. T.; Mann, J. B. *Acta Crystallogr., Sect. A* **1968**, *A24*, 321.

(21) Stewart, R. F.; Davidson, E. R.; Simpson, W. T. *J. Chem. Phys.* **1965**, *42*, 3175.

(22) Cromer, D. T. *Acta Crystallogr., Sect. A* **1965**, *A18*, 17.

(23) Siiman, O.; Titus, D. D.; Cowman, C. D.; Fresco, J.; Gray, H. B. *J. Am. Chem. Soc.* **1974**, *96*, 2353.

(24) Fay, R. C.; Pinnavaia, T. J. *Inorg. Chem.* **1968**, *7*, 508.

Table II. Final Atomic Fractional Coordinates for  $[\text{Zr}(\text{Sacac})_4]^a$ 

atom	$10^4x$	$10^4y$	$10^4z$
Zr	2942.7 (5)	6171.8 (2)	2876.4 (4)
S <sub>a</sub>	1843 (2)	5375.9 (6)	1495 (1)
S <sub>b</sub>	6 (2)	6389.2 (7)	2230 (1)
S <sub>c</sub>	2879 (2)	6524.0 (6)	680 (1)
S <sub>d</sub>	3078 (2)	7233.4 (5)	2798 (1)
O <sub>a</sub>	3011 (4)	5470 (1)	3897 (3)
O <sub>b</sub>	1722 (4)	6366 (1)	4442 (3)
O <sub>c</sub>	5057 (4)	5877 (1)	2201 (3)
O <sub>d</sub>	4774 (4)	6377 (1)	4121 (3)
C <sub>a1</sub>	2584 (8)	4854 (3)	5352 (5)
C <sub>a2</sub>	2334 (6)	5050 (2)	4150 (4)
C <sub>a3</sub>	1414 (7)	4751 (2)	3377 (5)
C <sub>a4</sub>	1205 (6)	4846 (2)	2226 (5)
C <sub>a5</sub>	369 (8)	4434 (2)	1502 (6)
C <sub>b1</sub>	865 (7)	6770 (3)	6112 (5)
C <sub>b2</sub>	754 (6)	6689 (2)	4837 (4)
C <sub>b3</sub>	-432 (6)	6948 (2)	4196 (5)
C <sub>b4</sub>	-874 (6)	6820 (2)	3111 (5)
C <sub>b5</sub>	-2349 (7)	7071 (3)	2608 (5)
C <sub>c1</sub>	6968 (7)	5298 (3)	1532 (5)
C <sub>c2</sub>	5683 (6)	5695 (2)	1327 (4)
C <sub>c3</sub>	5269 (6)	5845 (3)	209 (4)
C <sub>c4</sub>	4185 (6)	6207 (2)	-123 (4)
C <sub>c5</sub>	4065 (8)	6353 (3)	-1384 (5)
C <sub>d1</sub>	6165 (7)	6504 (3)	5829 (4)
C <sub>d2</sub>	5102 (6)	6717 (2)	4896 (4)
C <sub>d3</sub>	4602 (6)	7238 (2)	4902 (4)
C <sub>d4</sub>	3789 (6)	7496 (2)	4042 (4)
C <sub>d5</sub>	3527 (9)	8083 (2)	4152 (6)

<sup>a</sup> Numbers in parentheses are estimated standard deviations in the last significant figure.

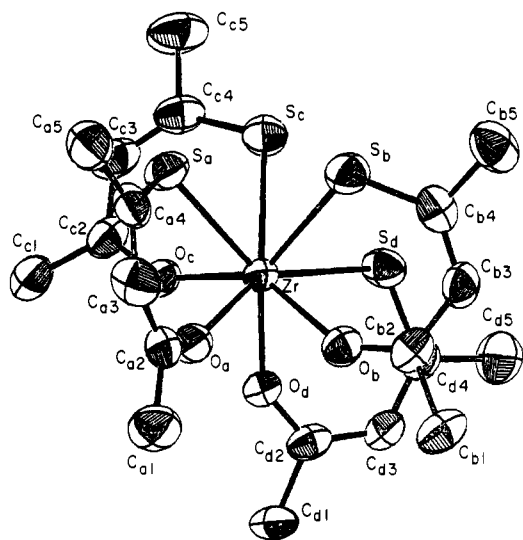


Figure 1. Model in perspective of the  $[\text{Zr}(\text{Sacac})_4]$  molecule viewed along the quasi-8 axis of the  $\text{ZrS}_4\text{O}_4$  coordination group. Each atom is represented by a 50% probability thermal ellipsoid consistent with the thermal parameters in Table III.

carbamato)zirconium(IV) complexes ( $353\text{--}359\text{ cm}^{-1}$ ).<sup>10</sup> On the other hand, it is possible that  $\nu(\text{Zr-S})$  in  $[\text{Zr}(\text{Sacac})_4]$  lies below the  $300\text{-cm}^{-1}$  limit of our spectrophotometer since calculated  $\nu(\text{M-S})$  frequencies for  $\text{M}(\text{Sacac})_2$  complexes are in the range  $185\text{--}285\text{ cm}^{-1}$ .<sup>18,23</sup>

**Solid-State Structure of  $[\text{Zr}(\text{Sacac})_4]$ .** Final atomic coordinates and thermal parameters for  $[\text{Zr}(\text{Sacac})_4]$  are presented in Tables II and III.<sup>25</sup> A table of observed and calculated structure factor amplitudes is available.<sup>25</sup> Perspective views showing the molecular geometry and the atom-numbering scheme are presented in Figures 1 and 2; atoms of the four

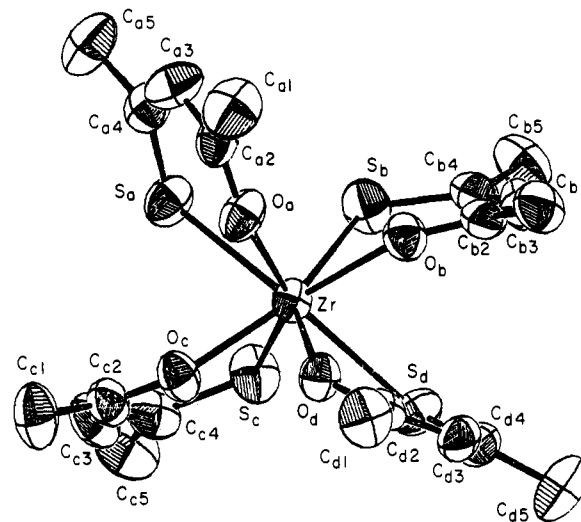


Figure 2. Model in perspective of the  $[\text{Zr}(\text{Sacac})_4]$  molecule viewed, approximately, along the quasi-twofold axis perpendicular to the quasi-8 axis of the  $\text{ZrS}_4\text{O}_4$  coordination group. Each atom is represented by a 50% probability thermal ellipsoid consistent with the thermal parameters in Table III.

Table IV. Bond Distances in the Coordination Group of  $[\text{Zr}(\text{Sacac})_4]^a$ 

Zr-O <sub>A</sub>	length, Å	Zr-O <sub>B</sub>	length, Å
Zr-O <sub>b</sub>	2.199 (3)	Zr-O <sub>a</sub>	2.132 (3)
Zr-O <sub>d</sub>	2.171 (3)	Zr-O <sub>c</sub>	2.132 (3)
av <sup>b</sup>	2.185 (3, 14)	av <sup>b</sup>	2.132 (3, 0)
Zr-S <sub>A</sub>	length, Å	Zr-S <sub>B</sub>	length, Å
Zr-S <sub>a</sub>	2.723 (2)	Zr-S <sub>b</sub>	2.660 (2)
Zr-S <sub>c</sub>	2.725 (2)	Zr-S <sub>d</sub>	2.670 (2)
av <sup>b</sup>	2.724 (2, 1)	av <sup>b</sup>	2.665 (2, 5)

<sup>a</sup> Numbers in parentheses are estimated standard deviations in the last significant figure. <sup>b</sup> The numbers in parentheses following each averaged value are the root-mean-square estimated standard deviations for an individual datum and the mean deviation from the averaged value.

Table V. Polyhedral Edge Lengths and Bond Angles Subtended at the Zr(IV) Atom in the Coordination Group of  $[\text{Zr}(\text{Sacac})_4]^a$ 

edge type <sup>b</sup>	atoms	length, Å	atoms	angle, deg
<i>s<sub>r</sub></i>	S <sub>a</sub> ···O <sub>a</sub> <sup>c</sup>	2.972 (4)	S <sub>a</sub> -Zr-O <sub>a</sub>	74.37 (9)
<i>s<sub>r</sub></i>	S <sub>b</sub> ···O <sub>b</sub> <sup>c</sup>	2.944 (4)	S <sub>b</sub> -Zr-O <sub>b</sub>	73.91 (9)
<i>s<sub>r</sub></i>	S <sub>c</sub> ···O <sub>c</sub> <sup>c</sup>	3.015 (4)	S <sub>c</sub> -Zr-O <sub>c</sub>	75.66 (9)
<i>s<sub>r</sub></i>	S <sub>d</sub> ···O <sub>d</sub> <sup>c</sup>	3.001 (4)	S <sub>d</sub> -Zr-O <sub>d</sub>	75.83 (9)
<i>s</i>	S <sub>a</sub> ···S <sub>b</sub>	3.128 (2)	S <sub>a</sub> -Zr-S <sub>b</sub>	71.03 (5)
<i>s</i>	S <sub>c</sub> ···S <sub>d</sub>	3.059 (2)	S <sub>c</sub> -Zr-S <sub>d</sub>	69.07 (5)
<i>s</i>	O <sub>a</sub> ···O <sub>b</sub>	2.596 (5)	O <sub>a</sub> -Zr-O <sub>b</sub>	73.63 (13)
<i>s</i>	O <sub>c</sub> ···O <sub>d</sub>	2.598 (4)	O <sub>c</sub> -Zr-O <sub>d</sub>	74.28 (12)
<i>l</i>	S <sub>b</sub> ···S <sub>c</sub>	3.125 (2)	S <sub>b</sub> -Zr-S <sub>c</sub>	70.93 (5)
<i>l</i>	O <sub>a</sub> ···O <sub>d</sub>	2.741 (5)	O <sub>a</sub> -Zr-O <sub>d</sub>	79.15 (13)
<i>l</i>	S <sub>a</sub> ···O <sub>c</sub>	3.114 (4)	S <sub>a</sub> -Zr-O <sub>c</sub>	78.75 (9)
<i>l</i>	S <sub>d</sub> ···O <sub>b</sub>	3.157 (4)	S <sub>d</sub> -Zr-O <sub>b</sub>	80.22 (9)
<i>l</i>	S <sub>a</sub> ···S <sub>c</sub>	3.173 (2)	S <sub>a</sub> -Zr-S <sub>c</sub>	71.24 (5)
<i>l</i>	S <sub>b</sub> ···S <sub>d</sub>	3.427 (2)	S <sub>b</sub> -Zr-S <sub>d</sub>	80.04 (5)
<i>l</i>	O <sub>a</sub> ···O <sub>c</sub>	2.882 (5)	O <sub>a</sub> -Zr-O <sub>c</sub>	85.04 (13)
<i>l</i>	O <sub>b</sub> ···O <sub>d</sub>	2.653 (5)	O <sub>b</sub> -Zr-O <sub>d</sub>	74.76 (12)

<sup>a</sup> Numbers in parentheses are estimated standard deviations in the last significant figure. <sup>b</sup> The edges of the square faces of the antiprism are labeled *s<sub>r</sub>*, if they are spanned by a bidentate ligand, or *s*, if they are not spanned by a ligand. The *l* edges are the lateral edges that connect the square faces. <sup>c</sup> The "bite" of the ligand.

thioacetylacetonate ligands are distinguished by a literal subscript (a, b, c, or d). Bond distances, polyhedral edge lengths, and bond angles in the  $\text{ZrS}_4\text{O}_4$  coordination group

(25) See paragraph at the end of paper regarding supplementary material.

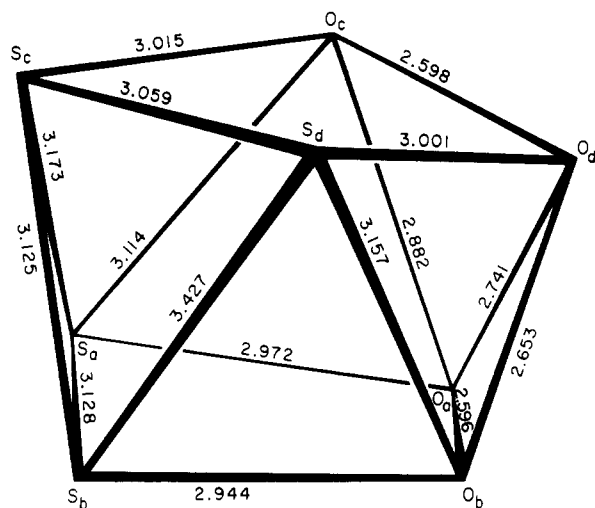


**Figure 3.** Perspective view (adapted from a computer-drawn diagram) of the distorted-square-antiprismatic coordination polyhedron in  $\text{Zr}(\text{Sacac})_4$ .

are listed in Tables IV and V. A perspective view of the coordination polyhedron is illustrated in Figure 3.

The crystal contains discrete eight-coordinate molecules in which the bidentate thioacetylacetonate ligands span the *s* edges of a (necessarily distorted)  $D_{4d}$ - $\bar{8}2m$  square antiprism. The unsymmetrical ligands are arranged so as to cluster the four sulfur atoms in all-cis positions on two adjacent triangular faces of the coordination polyhedron (cf. Figure 3). Thus, the observed stereoisomer may be described as the *ssss*- $C_2$  square-antiprismatic isomer, where the quasi-twofold axis bisects the  $\text{O}_a\text{ZrO}_d$  and  $\text{S}_b\text{ZrS}_c$  angles (cf. Figures 1 and 2).

The structure of  $[\text{Zr}(\text{Sacac})_4]$  is obviously related to the *ssss*- $D_2$  square-antiprismatic structure of  $[\text{Zr}(\text{acac})_4]$ ,<sup>26</sup> but the coordination polyhedron in the thioacetylacetonate complex is much more distorted. Because the larger sulfur atoms are clustered on one side of the molecule, the two quadrilateral faces of the antiprism are not parallel; the dihedral angle between the faces defined by atoms  $\text{S}_a, \text{S}_b, \text{O}_b,$  and  $\text{O}_a$  and by atoms  $\text{S}_c, \text{S}_d, \text{O}_d,$  and  $\text{O}_c$  (cf. Figure 3) is  $7.2^\circ$ . Moreover, the quadrilateral faces exhibit significant departures from planarity due to folding about the diagonals  $\text{O}_a\cdots\text{S}_b$  and  $\text{O}_c\cdots\text{S}_d$ . Atoms  $\text{S}_a, \text{S}_b, \text{O}_b,$  and  $\text{O}_a$  deviate from the least-squares mean plane (Table IX) by an average distance of  $0.070 \text{ \AA}$  owing to a  $7.6^\circ$  fold about  $\text{O}_a\cdots\text{S}_b$ , while atoms  $\text{S}_c, \text{S}_d, \text{O}_d,$  and  $\text{O}_c$  exhibit an average deviation from planarity of  $0.131 \text{ \AA}$  due to a  $14.0^\circ$  fold about  $\text{O}_c\cdots\text{S}_d$ . The diagonals of the quadrilateral faces about which folding occurs,  $\text{O}_a\cdots\text{S}_b$  ( $3.932 \text{ \AA}$ ) and  $\text{O}_c\cdots\text{S}_d$  ( $3.878 \text{ \AA}$ ), are  $0.3\text{--}0.4 \text{ \AA}$  shorter than the other diagonals,  $\text{S}_a\cdots\text{O}_b$  ( $4.266 \text{ \AA}$ ) and  $\text{S}_c\cdots\text{O}_d$  ( $4.321 \text{ \AA}$ ).

The distortion of the coordination polyhedron in  $[\text{Zr}(\text{Sacac})_4]$  is conveniently discussed in terms of distortion pathways<sup>27</sup> which interconvert the  $D_{4d}$  square antiprism,  $C_{2v}$  bicapped trigonal prism, and  $D_{2d}$  dodecahedron (Figure 4). The observed folding about the square-antiprismatic face diagonals  $\text{O}_a\cdots\text{S}_b$  and  $\text{O}_c\cdots\text{S}_d$  takes the antiprism in the direction of a  $D_{2d}$  dodecahedron having *b* edges  $\text{O}_a\cdots\text{S}_b, \text{O}_c\cdots\text{S}_d, \text{O}_a\cdots\text{O}_c,$  and  $\text{S}_b\cdots\text{S}_d$ ; therefore the two BAAB trapezoids of the dodecahedron are defined by  $\text{S}_b, \text{O}_b, \text{O}_d,$  and  $\text{O}_c$  and by  $\text{S}_d, \text{S}_c, \text{S}_a,$  and  $\text{O}_a$ , and the corresponding dodecahedral stereoisomer is the *mmgg*- $C_1$  isomer.<sup>28</sup> However, the observed structure is far from the dodecahedral limit; the dihedral angle

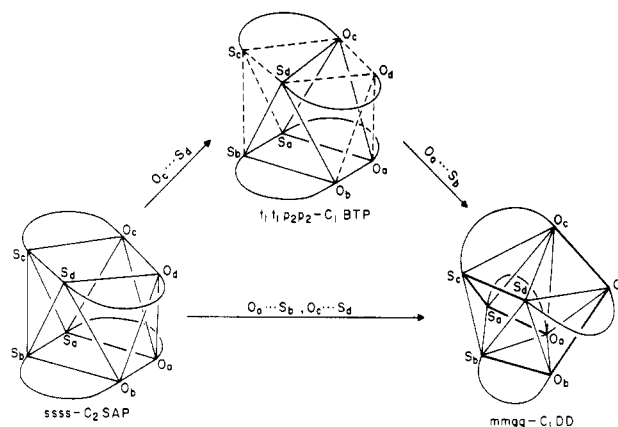


**Figure 4.** Idealized distortion pathways that interconvert the square antiprism (SAP), bicapped trigonal prism (BTP), and dodecahedron (DD). The distortions involve folding about and compression along the indicated diagonals of the quadrilateral faces ( $\text{O}_a\cdots\text{S}_b$  and/or  $\text{O}_c\cdots\text{S}_d$ ). The BAAB trapezoids of the dodecahedron are indicated with heavy lines, and the stereoisomers shown are appropriate for the ligand wrapping pattern observed in  $[\text{Zr}(\text{Sacac})_4]$ .

**Table VI.**  $\delta$  and  $\varphi$  Parameters (Deg) for  $[\text{Zr}(\text{Sacac})_4]$  and Theoretical Values for Idealized Eight-Coordination Polyhedra<sup>a</sup>

$[\text{Zr}(\text{Sacac})_4]$	theor values <sup>b</sup>		
	$D_{4d}^c$	$C_{2v}^d$	$D_{2d}^e$
$\delta(\text{O}_a\cdots\text{S}_b) = 7.6$	$\delta$ 0.0	0.0	29.5
$\delta(\text{O}_c\cdots\text{S}_d) = 14.0$	$\delta$ 0.0	21.8	29.5
$\delta(\text{O}_a\cdots\text{O}_c) = 39.0$	$\delta$ 52.4	48.2	29.5
$\delta(\text{S}_b\cdots\text{S}_d) = 52.4$	$\delta$ 52.4	48.2	29.5
$\varphi(\text{S}_b, \text{O}_b, \text{O}_d, \text{O}_c) = 18.6$	$\varphi$ 24.5	14.1	0.0
$\varphi(\text{S}_d, \text{S}_c, \text{S}_a, \text{O}_a) = 15.8$	$\varphi$ 24.5	14.1	0.0

<sup>a</sup>  $\delta(\text{O}_a\cdots\text{S}_b)$  is the dihedral angle between the two triangular faces that join along the dodecahedral *b* edge  $\text{O}_a\cdots\text{S}_b$ .  $\varphi(\text{S}_b, \text{O}_b, \text{O}_d, \text{O}_c)$  is a measure of the nonplanarity of the trapezoid defined by  $\text{S}_b, \text{O}_b, \text{O}_d,$  and  $\text{O}_c$ . It is the dihedral angle between the plane defined by  $\text{S}_b, \text{O}_c,$  and the midpoint of  $\text{O}_b$  and  $\text{O}_d$ , and the plane defined by  $\text{O}_b, \text{O}_d,$  and the midpoint of  $\text{S}_b$  and  $\text{O}_c$ . <sup>b</sup> References 27 and 29. <sup>c</sup> Square antiprism. <sup>d</sup> Bicapped trigonal prism. <sup>e</sup> Dodecahedron.

between the mean planes of the two BAAB trapezoids is  $85.2^\circ$  ( $90^\circ$  for a perfect dodecahedron), and the atoms that define the trapezoids depart from planarity by an average distance of  $0.25 \text{ \AA}$  (cf. Table IX). The location of the observed structure along the distortion pathway (Figure 4) can be estimated in terms of the  $\delta$  and  $\varphi$  shape parameters introduced by Porai-Koshits and Aslanov.<sup>29</sup> These parameters, listed and defined in Table VI, measure the extent to which an observed coordination polyhedron approximates one of the idealized polyhedra. On the basis of the extent of folding of the quadrilateral faces of the antiprism ( $\delta(\text{O}_a\cdots\text{S}_b) = 7.6^\circ$ ;  $\delta(\text{O}_c\cdots\text{S}_d) = 14.0^\circ$ ;  $\delta(\text{av}) = 10.8^\circ$ ), the observed structure lies  $\sim 35\%$  of the way along the distortion pathway between the square-antiprismatic *ssss*- $C_2$  stereoisomer and the dodecahedral *mmgg*- $C_1$  stereoisomer. However, this description oversimplifies the actual distortion since the two quadrilateral faces of the antiprism are folded by different amounts. If the smaller  $\delta$  angle,  $\delta(\text{O}_a\cdots\text{S}_b)$ , were  $0^\circ$ , corresponding to one flat quadrilateral face ( $\text{S}_a, \text{S}_b, \text{O}_b, \text{O}_a$ ), then the larger  $\delta$  angle,  $\delta(\text{O}_c\cdots\text{S}_d)$ , of  $14.0^\circ$  would indicate that the observed structure lies  $\sim 65\%$  of the way along the distortion pathway between the square-antiprismatic *ssss*- $C_2$  stereoisomer and the bicapped-trigonal-prismatic  $t_1t_1p_2p_2$ - $C_1$  stereoisomer<sup>30</sup> (cf. Figure

(26) Silverton, J. V.; Hoard, J. L. *Inorg. Chem.* **1963**, *2*, 243.

(27) Muettterties, E. L.; Guggenberger, L. J. *J. Am. Chem. Soc.* **1974**, *96*, 1748.

(28) For a description of dodecahedral edge and vertex nomenclature, see: Hoard, J. L.; Silverton, J. V. *Inorg. Chem.* **1963**, *2*, 235.

(29) Porai-Koshits, M. A.; Aslanov, L. A. *J. Struct. Chem. (Engl. Transl.)* **1972**, *13*, 244.

(30) The edge nomenclature for the bicapped trigonal prism is defined in ref 29.

Table VII. Thioacetylacetonate Ligand Dimensions in  $[\text{Zr}(\text{Sacac})_4]^a$ 

atoms	ligand a	ligand b	ligand c	ligand d	$av^b$
(a) Distances, Å					
$\text{S} \cdots \text{O}^c$	2.972 (4)	2.944 (4)	3.015 (4)	3.001 (4)	2.983 (4, 25, 39)
$\text{O}-\text{C}_2$	1.243 (6)	1.260 (6)	1.259 (5)	1.273 (6)	1.259 (6, 8, 16)
$\text{S}-\text{C}_4$	1.684 (6)	1.690 (6)	1.686 (6)	1.698 (5)	1.689 (6, 5, 9)
$\text{C}_2-\text{C}_3$	1.402 (8)	1.404 (8)	1.399 (7)	1.377 (7)	1.396 (8, 10, 19)
$\text{C}_3-\text{C}_4$	1.379 (8)	1.357 (7)	1.349 (8)	1.370 (7)	1.364 (8, 11, 15)
$\text{C}_1-\text{C}_2$	1.504 (8)	1.511 (7)	1.499 (8)	1.499 (7)	1.503 (8, 4, 8)
$\text{C}_4-\text{C}_5$	1.506 (8)	1.515 (8)	1.525 (8)	1.497 (8)	1.511 (8, 9, 14)
(b) Angles, Deg					
$\text{Zr}-\text{O}-\text{C}_2$	146.2 (4)	141.9 (3)	144.9 (3)	141.1 (3)	143.5 (3, 20, 27)
$\text{Zr}-\text{S}-\text{C}_4$	112.8 (2)	113.1 (2)	112.5 (2)	111.9 (2)	112.6 (2, 4, 7)
$\text{O}-\text{C}_2-\text{C}_1$	116.7 (5)	115.5 (5)	116.1 (5)	113.4 (5)	115.4 (5, 10, 20)
$\text{S}-\text{C}_4-\text{C}_5$	114.3 (4)	114.3 (4)	113.9 (5)	113.9 (4)	114.1 (4, 2, 2)
$\text{O}-\text{C}_2-\text{C}_3$	123.8 (5)	125.0 (5)	124.5 (5)	125.4 (5)	124.7 (5, 5, 9)
$\text{S}-\text{C}_4-\text{C}_3$	127.1 (4)	127.6 (4)	128.3 (4)	127.6 (4)	127.6 (4, 3, 7)
$\text{C}_1-\text{C}_2-\text{C}_3$	119.5 (5)	119.4 (5)	119.4 (5)	121.1 (5)	119.9 (5, 6, 12)
$\text{C}_3-\text{C}_4-\text{C}_5$	118.6 (5)	118.1 (5)	117.8 (5)	118.4 (5)	118.2 (5, 3, 4)
$\text{C}_2-\text{C}_3-\text{C}_4$	126.5 (5)	124.7 (5)	127.1 (5)	126.6 (5)	126.2 (5, 8, 15)
(c) Fold of the Chelate Ring about $\text{S} \cdots \text{O}$ , Deg					
$\alpha^d$	-21.1	27.9	17.3	25.5	

<sup>a</sup> Numbers in parentheses are estimated standard deviations in the last significant figure. <sup>b</sup> The numbers in parentheses following each averaged value are the root-mean-square estimated standard deviation for an individual datum and the mean and the maximum deviation from the average value. <sup>c</sup> The "bite" of the ligand. <sup>d</sup> Dihedral angle between the planes  $\text{ZrSO}$  and  $\text{SC}_2\text{C}_3\text{C}_4\text{O}$ . A positive value indicates that the ligand is folded away from the quasi- $\bar{z}$  axis of the square antiprism.

4). In the bicapped-trigonal-prismatic isomer, the capping sites are occupied by atoms  $\text{S}_c$  and  $\text{O}_d$ . Thus, the actual distortion is a hybrid of the idealized distortions shown in Figure 4, with the observed coordination polyhedron lying closer to the square antiprism and bicapped trigonal prism than to the dodecahedron. We find it convenient to describe the coordination polyhedron in terms of the higher symmetry polyhedron and will refer to it as a distorted square antiprism.

It is interesting to compare the coordination polyhedron in  $[\text{Zr}(\text{Sacac})_4]$  with coordination polyhedra in  $[\text{M}(\text{acac})_4]$  complexes.<sup>31</sup> The acetylacetonates are found in two crystalline forms ( $\alpha$  and  $\beta$ ), typified by  $\beta$ - $[\text{Zr}(\text{acac})_4]$ <sup>26</sup> and  $\alpha$ - $[\text{Th}(\text{acac})_4]$ .<sup>32</sup> The coordination polyhedron in  $[\text{Zr}(\text{acac})_4]$  closely approximates a square antiprism, both quadrilateral faces being folded by only  $3.2^\circ$ ,<sup>31</sup> while the coordination polyhedron in  $[\text{Th}(\text{acac})_4]$  is best described as a bicapped trigonal prism. In  $[\text{Th}(\text{acac})_4]$  one quadrilateral face is folded by  $19.8^\circ$  and the other (the "square" face) by  $5.4^\circ$ .<sup>31</sup> Thus, the coordination polyhedron in  $[\text{Zr}(\text{Sacac})_4]$  has features common to the coordination polyhedra in both  $[\text{M}(\text{acac})_4]$  crystalline forms. Note, however, that the stereoisomers in the  $[\text{Zr}(\text{Sacac})_4]$  and  $[\text{M}(\text{acac})_4]$  systems differ somewhat, owing to a difference in the face diagonals about which the folding occurs.  $[\text{Zr}(\text{acac})_4]$  lies  $\sim 10\%$  of the way along the distortion pathway between the square-antiprismatic  $ssss-D_2$  stereoisomer and the dodecahedral  $mmmm-D_{2d}$  stereoisomer, while  $[\text{Th}(\text{acac})_4]$  exists as the  $h_1h_1p_2p_2-C_2$  stereoisomer.

Distortion of  $[\text{Zr}(\text{Sacac})_4]$  from the square-antiprismatic  $ssss-C_2$  stereoisomer toward the dodecahedral  $mmgg-C_1$  stereoisomer is also evidenced by bond distances and polyhedral edge lengths in the coordination group. Both the  $\text{Zr}-\text{O}$  and the  $\text{Zr}-\text{S}$  distances fall into two groups (cf. Table IV) in accord with the sites (A or B) that the oxygen and sulfur atoms would occupy in the limiting dodecahedron (cf. Figure 4). The bonds to the dodecahedral A sites (average  $\text{Zr}-\text{O}_A$ , 2.185 Å; average  $\text{Zr}-\text{S}_A$ , 2.724 Å) are significantly longer than the bonds to the B sites (average  $\text{Zr}-\text{O}_B$ , 2.132 Å; average  $\text{Zr}-\text{S}_B$ , 2.665 Å), as is usually the case in genuine dodecahedral structures.<sup>33</sup>

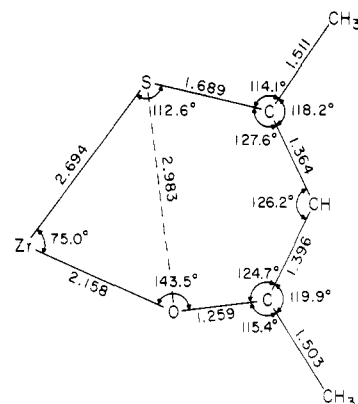


Figure 5. Averaged bond distances and angles in the thioacetylacetonate ligands. Deviations from the average are given in Tables IV and VII.

The averaged length of all four  $\text{Zr}-\text{O}$  bonds in  $[\text{Zr}(\text{Sacac})_4]$  (2.158 Å) is 0.040 Å less than the averaged  $\text{Zr}-\text{O}$  bond length in  $[\text{Zr}(\text{acac})_4]$  (2.198 Å)<sup>26</sup> and also less than the averaged  $\text{Zr}-\text{O}$  bond distances in  $[\text{Zr}(\text{bzbz})_4]$  (bzbz = dibenzoylmethane) (2.172 Å)<sup>36</sup> and  $[\text{Zr}(\text{SOCNET}_2)_4]$  (2.190 Å).<sup>14</sup> The  $\text{Zr}-\text{O}$  bonds in  $[\text{Zr}(\text{Sacac})_4]$  appear to be shortened at the expense of the  $\text{Zr}-\text{S}$  bonds; the averaged length of all four  $\text{Zr}-\text{S}$  bonds (2.694 Å) is 0.015 Å greater than the averaged  $\text{Zr}-\text{S}$  bond length in  $[\text{Zr}(\text{SOCNET}_2)_4]$  (2.679 Å).<sup>14</sup> Also consistent with a distortion of  $[\text{Zr}(\text{Sacac})_4]$  toward the dodecahedral  $mmgg-C_1$  stereoisomer is the fact that the longest  $\text{O} \cdots \text{O}$  and  $\text{S} \cdots \text{S}$  edges ( $\text{O}_a \cdots \text{O}_c$ , 2.882 Å;  $\text{S}_b \cdots \text{S}_d$ , 3.427 Å; cf. Figure 3 and Table V) correspond to  $b$  edges in the limiting dodecahedron (cf. Figure 4). The remaining four  $\text{O} \cdots \text{O}$  edges are 0.1–0.2 Å less than the  $\text{O} \cdots \text{O}$  van der Waals contact (2.80 Å),<sup>37</sup> and the remaining four  $\text{S} \cdots \text{S}$  edges are 0.3–0.4 Å less than the  $\text{S} \cdots \text{S}$  van der Waals contact (3.45 Å).<sup>38</sup> These

(31) Steffen, W. L.; Fay, R. C. *Inorg. Chem.* **1978**, *17*, 779.

(32) Allard, B. *Acta Chem. Scand., Ser. A* **1976**, *A30*, 461.

(33)  $[\text{Zr}(\text{acac})_2(\text{NO}_3)_2]$ ,<sup>34</sup>  $[\text{Zr}(\text{acac})_3(\text{NO}_3)]$ ,<sup>35</sup> and  $[\text{Zr}(\text{SOCNET}_2)_4]$ <sup>14</sup> are examples.

(34) Day, V. W.; Fay, R. C. *J. Am. Chem. Soc.* **1975**, *97*, 5136.

(35) Muller, E. G.; Day, V. W.; Fay, R. C. *J. Am. Chem. Soc.* **1976**, *98*, 2165.

(36) Chun, H. K.; Steffen, W. L.; Fay, R. C. *Inorg. Chem.* **1979**, *18*, 2458.

(37) Pauling, L. "The Nature of the Chemical Bond", 3rd ed.; Cornell University Press: Ithaca, NY, 1960; p 260.

(38) van der Helm, D.; Lessor, A. E., Jr.; Merritt, L. L., Jr. *Acta Crystallogr.* **1962**, *15*, 1227.

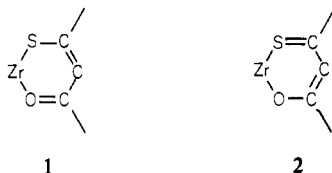
Table VIII. Selected Bond Distances in  $[M(\text{RCOCHCSR})_n]$  Complexes

compd	R	C $\rightarrow$ O	C $\rightarrow$ S	C $\rightarrow$ C(O)	C $\rightarrow$ C(S)	S $\rightarrow$ O <sup>a</sup>	ref
[Zr(Sacac) <sub>4</sub> ]	Me	1.259	1.689	1.396	1.364	2.983	this work
[Ni(Sacac) <sub>2</sub> ]	Me	1.264	1.698	1.406	1.360	2.998	23
[Ni(Sdpm) <sub>2</sub> ]	<i>t</i> -Bu	1.264	1.708	1.439	1.363	2.966	40
[Pd(Sdpm) <sub>2</sub> ]	<i>t</i> -Bu	1.260	1.707	1.421	1.380	3.148	41
[Pd(Sbzbz) <sub>2</sub> ] <sup>b</sup>	Ph	1.22	1.74	1.42	1.34	3.16	42
[Pd( $\eta^3$ -C <sub>4</sub> H <sub>7</sub> )(Sbzbz)]	Ph	1.26	1.712	1.41	1.40	3.237	43
[Fe(Sbzbz) <sub>3</sub> ]	Ph	1.259	1.705	1.403	1.378	3.037	44

<sup>a</sup> The "bite" of the ligand. <sup>b</sup> This structure was determined by photographic methods, and esd's are large (0.04–0.05 Å).

distances are indicative of considerable crowding in the coordination group, due in part to the relatively large bite of the thioacetylacetonate ligand (average 2.983 Å). The normalized bite of the ligand (1.230, in units of the mean metal-donor atom distance) is slightly larger than that in [Zr(acac)<sub>4</sub>] (1.217) but is still in the range where the *ssss* stereoisomer is expected to be one of the most stable of the possible square-antiprismatic and dodecahedral stereoisomers.<sup>39</sup>

Bond lengths and bond angles within the thioacetylacetonate ligands are presented in Table VII, and averaged values are summarized in Figure 5. Except for the ligand bite, deviations from the averaged values are statistically insignificant. Ligand dimensions agree well with those found in other thio- $\beta$ -diketonate structures;<sup>23,40–44</sup> selected bond distances in  $[M(\text{RCOCHCSR})_n]$  complexes in which both R groups are the same are compared in Table VIII. In [Zr(Sacac)<sub>4</sub>], as in other thio- $\beta$ -diketonate structures, the C $\rightarrow$ C bond adjacent to C $\rightarrow$ S is slightly shorter than the C $\rightarrow$ C bond adjacent to C $\rightarrow$ O. This indicates that resonance structure 1 makes a greater contribution to the electronic structure than 2.



The five atoms of each C<sub>3</sub>SO thioacetylacetonate skeleton exhibit only minor departures from planarity; displacements from the C<sub>3</sub>SO mean planes are  $\leq 0.048$  Å (average displacement 0.021 Å; cf. Table IX). However, the Zr atom is displaced from the mean plane of each ligand by 0.5–0.9 Å, which implies that the chelate rings are appreciably folded about the S $\cdots$ O edges of the coordination polyhedron. The dihedral angles between the ligand planes and the planes defined by the appropriate S–Zr–O group are 21.1, 27.9, 17.3, and 25.5° for ligands a, b, c, and d, respectively. Ring a is folded so as to bend the ligand toward the quasi- $\delta$  axis of the antiprism, while ligands b, c, and d are bent away from the quasi- $\delta$  axis (cf. Figure 2). Ring folding in other thio- $\beta$ -diketonate structures varies from essentially no folding in [Ni(Sacac)<sub>2</sub>]<sup>23</sup> to a fold of 24.8° in one of the rings of [Fe(Sbzbz)<sub>3</sub>].<sup>44</sup> In the square-antiprismatic *ssss* stereoisomers of  $[M(\text{acac})_4]$  (M = Zr, Ce, U, or Np), the ligands invariably bend away from the quasi- $\delta$  axis (by  $\sim 23^\circ$ ).<sup>45</sup> This has been rationalized in terms of  $\pi$ -bonding interactions between the empty metal  $d_{z^2}$  orbital and  $\pi$ -donor orbitals on the ligands.<sup>46</sup> The folding of ring a in the opposite direction in the structure

Table IX. Least-Squares Mean Planes of the Form  $AX + BY + CZ = D^a$ 

Planes					
plane	atoms	A	B	C	D
1	S <sub>a</sub> , S <sub>b</sub> , O <sub>a</sub> , O <sub>b</sub>	0.7643	0.5469	-0.3417	7.8832
2	S <sub>c</sub> , S <sub>d</sub> , O <sub>c</sub> , O <sub>d</sub>	0.8388	0.4717	-0.2720	9.6778
3	O <sub>b</sub> , O <sub>d</sub> , O <sub>c</sub>	0.1938	0.9436	-0.2686	14.2462
4	S <sub>d</sub> , S <sub>c</sub> , S <sub>a</sub> , O <sub>a</sub>	0.9803	-0.1499	-0.1290	-0.4645
5	O <sub>a</sub> , S <sub>a</sub> , C <sub>a2</sub> , C <sub>a3</sub> , C <sub>a4</sub>	0.8233	-0.5249	-0.2159	-6.1993
6	O <sub>b</sub> , S <sub>b</sub> , C <sub>b2</sub> , C <sub>b3</sub> , C <sub>b4</sub>	0.6171	0.7264	-0.3026	10.8163
7	O <sub>c</sub> , S <sub>c</sub> , C <sub>c2</sub> , C <sub>c3</sub> , C <sub>c4</sub>	-0.6474	-0.7592	-0.0665	-14.0998
8	O <sub>d</sub> , S <sub>d</sub> , C <sub>d2</sub> , C <sub>d3</sub> , C <sub>d4</sub>	0.8630	0.2511	-0.4383	5.3062
Atoms and Their Displacements From Planes, A					
plane	displacements				
1	S <sub>a</sub> , 0.064; S <sub>b</sub> , -0.063; O <sub>a</sub> , -0.077; O <sub>b</sub> , 0.076 <sup>b</sup>				
2	S <sub>c</sub> , 0.121; S <sub>d</sub> , -0.119; O <sub>c</sub> , -0.143; O <sub>d</sub> , 0.141 <sup>b</sup>				
3	S <sub>b</sub> , -0.175; O <sub>b</sub> , 0.310; O <sub>d</sub> , -0.327; O <sub>c</sub> , 0.192				
4	S <sub>d</sub> , 0.202; S <sub>c</sub> , -0.297; S <sub>a</sub> , 0.294; O <sub>a</sub> , -0.198				
5	S <sub>a</sub> , 0.013; O <sub>a</sub> , -0.003; C <sub>a2</sub> , -0.008; C <sub>a3</sub> , 0.026; C <sub>a4</sub> , -0.028; C <sub>a1</sub> , -0.101; C <sub>a5</sub> , -0.188; Zr, 0.680				
6	S <sub>b</sub> , 0.003; O <sub>b</sub> , -0.024; C <sub>b2</sub> , 0.046; C <sub>b3</sub> , -0.040; C <sub>b4</sub> , 0.016; C <sub>b1</sub> , 0.324; C <sub>b5</sub> , 0.146; Zr, -0.908				
7	S <sub>c</sub> , -0.029; O <sub>c</sub> , 0.026; C <sub>c2</sub> , -0.020; C <sub>c3</sub> , -0.025, C <sub>c4</sub> , 0.048; C <sub>c1</sub> , -0.054; C <sub>c5</sub> , 0.191; Zr, -0.547				
8	S <sub>d</sub> , 0.000; O <sub>d</sub> , 0.011; C <sub>d2</sub> , -0.022; C <sub>d3</sub> , 0.021; C <sub>d4</sub> , -0.010; C <sub>d1</sub> , -0.163; C <sub>d5</sub> , -0.126; Zr, 0.813				
Interplanar Angles, Deg					
planes	angle	planes	angle		
1–2	7.2	3–4	85.2		

<sup>a</sup> X, Y, and Z are orthogonal coordinates measured in Å along a, b, and c\*, respectively, of the crystallographic coordinate system. <sup>b</sup> A displacement in the positive direction is toward Zr.

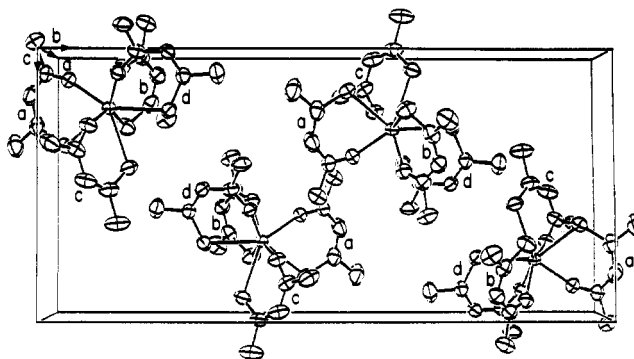


Figure 6. Model in perspective to illustrate the packing of [Zr(Sacac)<sub>4</sub>] molecules in the crystal. The contents of one unit cell are viewed normal to the (100) plane. The chelate rings are labeled a, b, c, or d.

of [Zr(Sacac)<sub>4</sub>] indicates that crystal-packing effects can be at least as important as  $\pi$ -bonding considerations in determining the direction of ring folding in square-antiprismatic

- (39) Blight, D. G.; Kepert, D. L. *Inorg. Chem.* **1972**, *11*, 1556.  
 (40) Coetzer, J.; Boeyens, J. C. A. *J. Cryst. Mol. Struct.* **1971**, *1*, 277.  
 (41) Pope, L. E.; Boeyens, J. C. A. *Acta Crystallogr., Sect. B* **1976**, *B32*, 1599.  
 (42) Shkol'nikova, L. M.; Yutal, Yu. M.; Shugam, E. A.; Knyazeva, A. N. *J. Struct. Chem. (Engl. Transl.)* **1973**, *14*, 80.  
 (43) Lippard, S. J.; Morehouse, S. M. *J. Am. Chem. Soc.* **1969**, *91*, 2504.  
 (44) Hoskins, B. F.; Pannan, C. D. *Inorg. Nucl. Chem. Lett.* **1975**, *11*, 409.  
 (45) Allard, B. *J. Inorg. Nucl. Chem.* **1976**, *38*, 2109.  
 (46) Burdett, J. K.; Hoffmann, R.; Fay, R. C. *Inorg. Chem.* **1978**, *17*, 2553.

chelates. The packing diagram in Figure 6 suggests that molecules related by an inversion center avoid close contacts between the atoms of their respective rings by bending the ligands away from each other toward their respective quasi-8 axes. The only intermolecular contacts in this structure that are appreciably shorter than the sum of the van der Waals radii involve methyl carbon atoms. There are six  $\text{CH}_3 \cdots \text{CH}_3$  contacts in the range 3.61–3.85 Å; the van der Waals contact for two methyl groups is 4.0 Å.<sup>37</sup>

**Stereochemistry and Fluxionality of  $[\text{Zr}(\text{Sacac})_4]$ .** The structures of the *mmmm*- $C_{2v}$  dodecahedral thiocarbamate complexes  $[\text{M}(\text{SOCNEt}_2)_4]$  ( $\text{M} = \text{Ti}$  and  $\text{Zr}$ )<sup>14</sup> provided the first evidence for clustering of sulfur atoms in eight-coordinate chelates that contain unsymmetrical sulfur-donor ligands. A similar clustering of sulfur atoms in  $[\text{Zr}(\text{Sacac})_4]$ , a complex that has a different coordination polyhedron (distorted square antiprism) and a different ligand wrapping pattern (*ssss*- $C_2$ ), suggests that sulfur-atom clustering may prove to be a common feature of higher-coordinate sulfur-ligand chelates.<sup>47</sup> From a geometrical point of view, a nonclustered arrangement with sulfur atoms trans to each other on both quadrilateral faces would have yielded an antiprism with more nearly square faces than exhibited by the observed clustered arrangement. To the extent that the observed coordination polyhedron is distorted toward a dodecahedron, one might have expected the sulfur and oxygen atoms to sort between the dodecahedral A and B sites, resulting in a nonclustered arrangement;  $\sigma$ -electronic effects,<sup>46</sup>  $\pi$ -electronic effects (Orgel's rule),<sup>15</sup> and steric effects<sup>28</sup> all predict donor atom sorting. In contrast, the dodecahedron toward which the observed structure is distorted (cf. Figure 4) has two sulfur atoms in A sites and two in B sites. It is relevant to observe that all square-planar bis- and octahedral tris(thio- $\beta$ -diketonate) complexes of known structure also exhibit a cis arrangement of sulfur atoms,<sup>23,40–42,44,48–51</sup> and weak, nonbonded S $\cdots$ S attractive forces have been suggested as a possible explanation.<sup>23,51</sup> In the  $[\text{M}(\text{SOCNEt}_2)_4]$  complexes, however, the S $\cdots$ S interactions were shown to be repulsive, and an alternate explanation, a trans influence of the sulfur atoms, was proposed to account for the all-cis stereochemistry.<sup>14</sup> The same explanation may apply to  $[\text{Zr}$ -

$(\text{Sacac})_4]$ . Clustering of sulfur atoms should not be expected in dodecahedral chelates where there is a large difference in the  $\pi$ -donor- $\pi$ -acceptor properties of the ligating atoms. A case in point is the structure of tetrakis(2-mercaptopyrimidinato)tungsten(IV),<sup>52</sup> where the four sulfur atoms occupy the A sites and four aromatic nitrogen atoms occupy the B sites in accord with Orgel's rule.

The 90-MHz  $^1\text{H}$  NMR spectra of  $[\text{Zr}(\text{Sacac})_4]$  in  $\text{CHClF}_2$  exhibit just two time-averaged methyl resonances in the temperature range  $-61$  to  $-163$  °C. These signals, separated by 24.3 Hz at  $-61$  °C, are due to the inequivalent acetyl and thioacetyl methyl groups. With decreasing temperature, the two resonances broaden smoothly from  $\sim 1$  Hz at  $-61$  °C to 4.3 Hz at  $-141$  °C, presumably due to increasing solvent viscosity. At  $-163$  °C, the lowest accessible temperature, the downfield resonance has a line width of 6.9 Hz, but the upfield signal is markedly broader, with a line width of  $\sim 14$  Hz. If the *ssss*- $C_2$  stereoisomer found in the solid state is the major species in solution, one would expect four methyl resonances of equal intensity in the slow-exchange limit. It is possible that a coalescence process is occurring in the temperature region  $-141$  to  $-163$  °C, with the coalescence temperature just below the limit of our measurements, or that the coalescence temperature is in the region  $-141$  to  $-163$  °C but is obscured by viscosity broadening. In any case, one can conclude that  $[\text{Zr}(\text{Sacac})_4]$  is at least as fluxional as  $[\text{Zr}(\text{acac})_4]$ , which has a coalescence temperature, in the same solvent, of  $-145$  °C; in the slow-exchange limit the *ssss*- $D_2$   $[\text{Zr}(\text{acac})_4]$  complex gives two methyl resonances of equal intensity separated by 11.1 Hz at 90 MHz.<sup>2,3</sup> Thus, clustering of sulfur atoms in  $[\text{Zr}(\text{Sacac})_4]$  does not appreciably slow the rate of rearrangement, as appears to be the case in  $[\text{Zr}(\text{SOCNMe}_2)_4]$ , where the coalescence temperature is  $-54$  °C,<sup>8</sup> the corresponding  $[\text{Zr}(\text{O}_2\text{CNMe}_2)_4]$  complex exhibits a single methyl proton resonance at  $-120$  °C.<sup>9</sup> The difference in the kinetic behavior of  $[\text{Zr}(\text{Sacac})_4]$  and  $[\text{Zr}(\text{SOCNMe}_2)_4]$  may be due to the difference in ligand bites in the six- and four-membered chelate rings. This point remains to be explored further.

**Acknowledgment.** We wish to thank the National Science Foundation for support of this research through Grants CHE-76-20300 and CHE-77-09756, the latter a departmental equipment grant that provided the X-ray diffractometer. M.E.S. thanks Dow Chemical for a fellowship.

**Registry No.**  $[\text{Zr}(\text{Sacac})_4]$ , 82648-59-7.

**Supplementary Material Available:** Listings of thermal parameters (Table III) and structure factor amplitudes (13 pages). Ordering information is given on any current masthead page.

(47) Note that the sulfur atoms are also clustered in all-cis positions in the seven-coordinate pentagonal-bipyramidal structure of  $[\text{Ti}(\text{SOCNEt}_2)_3\text{Cl}]$ : Hawthorne, S. L.; Fay, R. C. *J. Am. Chem. Soc.* **1979**, *101*, 5268.

(48) Kutschabsky, L.; Beyer, L. *Z. Chem.* **1971**, *11*, 30.

(49) Sieler, J.; Thomas, P.; Uhlemann, E.; Hohn, E. *Z. Anorg. Allg. Chem.* **1971**, *380*, 160.

(50) Craig, D. C.; Das, M.; Livingstone, S. E.; Stephenson, N. C. *Cryst. Struct. Commun.* **1974**, *3*, 283.

(51) Holm, R. H.; Gerlach, D. H.; Gordon, J. G., II; McNamee, M. G. *J. Am. Chem. Soc.* **1968**, *90*, 4184.

(52) Cotton, F. A.; Ilsley, W. H. *Inorg. Chem.* **1981**, *20*, 614.